

COMPARISON OF VIBRATION AND THERMAL PERFORMANCE AND SLIP OF V-BELTS

ZUZANA MURCINKOVA, JOZEF MASCENIK, TIBOR KRENICKY,
STEFAN GASPAR & JAN PASKO

*Technical University of Košice, Faculty of Manufacturing Technologies with seat in Prešov, Department of Designing and
Monitoring of Technical Systems, Bayerova 1, Prešov, Slovakia*

ABSTRACT

The study presents comparison of vibration and thermal performance of five tested V-belts by monitoring the vibrations and temperature by non-contact equipment. The various operating conditions were obtained by experimental laboratory setup. The range of revolutions was 600-3000 rpm. Two tensioning forces 400 and 700 N and loads of driven machine 0-100% were applied. Thus, V-belts operate under twenty-two running modes in which the vibrations and temperature were measured. The individual nature of V-belts running behaviour was compared and advantages and disadvantages are discussed. The best performance regarding vibration, temperature a temperature change is evaluated. Moreover, the belt slip as natural part of belt drive operation was analysed for one selected belt in terms of various revolutions and load under same tensioning force.

KEYWORDS: *Classical and Narrow Wedge, Cogged Belt, Pulley, Vibration, Temperature & Slip*

Received: Jan 10, 2020; **Accepted:** Jan 30, 2020; **Published:** Feb 06, 2020; **Paper Id.:** IJMPERDFEB202051

1. INTRODUCTION

A belt transmits a power and speed from prime mover (electric motor, engine) to the machine or by other words from one driver shaft to another driven shaft by use of pulleys. V-belt is one component of power transmission process. Using V-belts, the shaft distance is up to 2 metres. The amount of transmitted power is high what is achieved by moderate speed (comparing to flat belts with high speed but low power transmission). The power is transmitted by friction between the groove of pulley and belt. An amount of the transmitted power depends on the velocity of the belt, the arc of contact between belt and pulley and proper pre-tension in belt arranged on the pulleys, moreover, on conditions under which the belt is used (e.g. belt angular, offset misalignment), and on the material of the used belt.

The modern belts are belts with sophisticated shape and structure that creates the composite structure based on mainly elastomer materials and cords preferably made of steel. The configuration of composite structure is layered as the all cross-section can be divided into tension and compression parts and thus the requirements are different. Mainly compression part of V-belts cross-section can be made of wear protective and vibration absorption layers of various materials and compositions. The researchers bring the different internal belt structures and material composition patented in last decades to improve power and friction transmission, wear, heat and cold resistance and durability (see more in [1-4]).

Naturally, the power is lost when transmitted by belt driver and the efficiency is decreased. However, nowadays, reducing the power losses of engines has become a design matter [5]. In belt drives, the main sources of power loss are hysteresis effect of belt material, slip (relative sliding) of belt against pulley, transverse, torsional and longitudinal vibration of belt itself, and vibrations in bearings. Moreover, when belt slips, the heat start to built-up. Analysing the belt and belt drive performance, the mechanical load and also thermal load has to be considered as thermo mechanical laws [6] directly influence the efficiency of power transmission. The presented study measures and analyses the vibration of belt, temperature distribution and its change due to slip and hysteresis behaviour, and slip itself.

The materials of belts are preferably elastomers of viscoelastic behaviour characterized by hysteresis effects which are appropriate for damping of the mentioned belt vibrations occurring between driver and follower machines. On the other hand, the hysteresis is source of power loss due to bending, tension, shear, flank and radial compression phenomena that are cyclically repeated when belt is running. Bending deformation occurs when belt running on and off pulleys. Naturally, the tension occurs in belt as tensioning force is between both pulleys. Between individual layers of belt, the shear appears. The belt is compressed on the sides of pulley groove and flank compression occurs. Running the belt across the pulley, the normal (radial) force cause the radial load of belt.

In case of proper installation and maintenance, the belt drivers are effective and reliable power transmitters. In general, the belt drivers are of high efficiency and minimal maintenance and quick replacement, with relatively quiet operation. Furthermore, they reduce equipment repairs, minimize downtime and do not need lubrication. V-belt damps vibrations between diving and driven machines. Furthermore, they are protective as they do not allow to transmit overload.

A general demand for higher productivity results in wide range of different V-belts for specific applications. The frictional power transmission between pulleys through flexible elastic belts and the design of transmission systems which reduce the energy consumption are still problems of great interest for automobile and other industries [7].

V-belt transmits more power for same coefficient of friction (comparing to flat belt). The belt–pulley contact arcs consist of adhesion and sliding zones. Static friction exists in the adhesion zones, whereas kinetic friction exists in the sliding zones [8]. The three-dimensional frictional contact of the V-belt drive system is effected by angular speed. The effect of angular speed on the deformation of the V-belt and normal/tangential contact forces on the contact surfaces between the V-belt and pulley flange is estimated in [9].

The determination of slip of the belt is integral part of power transmission by belt. Slip of belt is quantity that affecting the efficiency of the belt transmission and it cannot be eliminated only minimized. Sometimes during the belt drive rotates, the friction force between belt and pulley is insufficient, the pulley/belt makes the forward motion without carrying belt/pulley. Thus, the velocities of both are not the same and belt slips. It can happen when high power from driver pulley cannot be transmitted by belt. Some researchers theoretically examined the slip behaviour in belt drives. Reynolds showed that torque transmissions between pulleys involved speed losses due to belt's elastic creep [10] appearing as a result of relative motion between belt and pulley due to changes in belt length when passing from the tight to slack side. Gerbert [11] explained the mechanism of slipping by dividing the arc of contact between belt and pulley into sticking (non-slipping) and slipping regions.

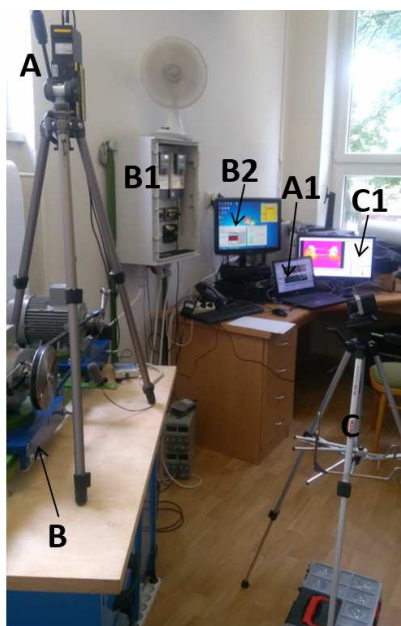
The presented study involves five specific commercial V-belts with aim to compare a vibration and thermal behaviour in various operating modes of measuring setup in laboratory conditions. Moreover, the study involves the

measurement of slip of V-belt regarding speed and percentage of load.

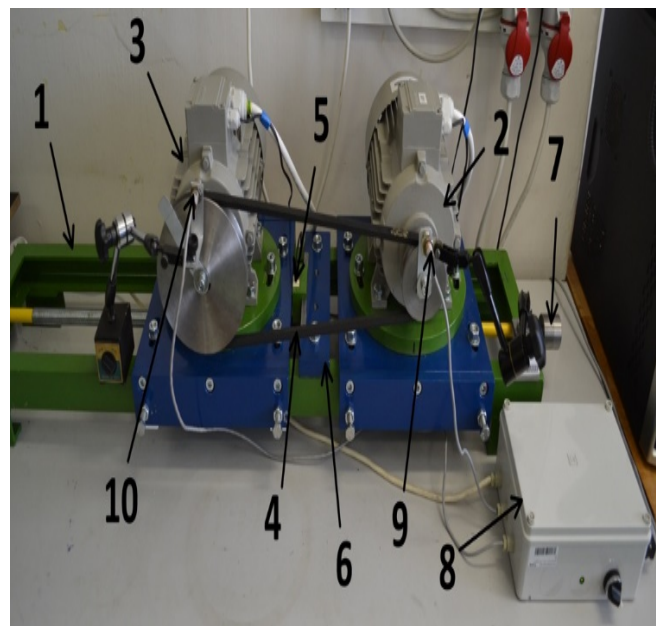
2. MEASUREMENT ARRANGEMENT

The described belt drive B in Figure 1a is component of measuring setup. The speed and load is control by Control and regulate unit B1. Software “Motor” B2 provides the information of tensioning force, actual speed of driving and driven electric motors, slip revolutions, coefficient of elastic slip. Moreover, the measuring setup involves the Polytec PDV 100, i.e. non-contact laser vibrometer A for measuring vibrational velocity of tested belt in lateral direction on upper i.e. slack (loose) side of belt. The mentioned vibrometer is single point vibrometer that is able to measure vibrational velocities in range up to 22kHz. The vibrational velocity and other quantities are measured and analysed by LabVIEW (Laboratory Virtual Instrumentation Engineering Workbench) software A1. The temperature distribution during individual operating modes is monitored by non-contact thermo-camera TIM450 C intended for industrial temperature monitoring with TIM Connect software.

The belt driver (Figure 1b) in measurement setup consists of a steel base frame 1, a pair of electric motors 2 and 3 placed on the slides mounted on the base frame. The necessary tension force is adjusted by the sliding the electric motors along frame 1. The belt tension is possible to control by means of a tensioning screw 7 located at the bottom of the frame and force sensor 5 and plate 6. The electric motor 2 serves as a driving electric motor, the other one 3 serves as a brake or load of driven machine. The driving and driven pulleys are of diameters 80 and 160 mm, respectively.



a



b

Measurement Setup: A – Polytec PDV 100 Vibrometer, A1 – LabVIEW Software, B – Belt Driver, B1 – Control and Regulate Unit, B2 –Motor Software, C – Thermo-Camera TIM450,C1 – TIM Connect Software

Belt Driver: 1 –Steel Frame, 2 - Driving Electric Motor, 3 - Electric Motor(Driven Motor) Simulating The Loading of Machine, 4 - Tested Belt, 5 –Force Sensor, 6 - Plate, 7 - Tensioning Screw, 8- Converter, 9- Sensor of Actual Revolutions of Driving Pulley, 10 - Sensor of Actual Revolutions of Driven Belt Pulley

Figure 1: Measurement Setup.

Three-phase electric motors from Siemens (1LA7090-2AA10ZA11 1,5KW 2900rpm, 400V 50Hz) were used for the drive. The electric motor on the driven pulley side represents a simulated driven devices as fans, pumps, machine tools

and the like, it means it counteracts. The transmission of the rotary movement between the pulleys located on the shafts of the electric motors is provided by a V-belt. The belt driver allows testing of various belts by simply replacing the pulleys on the motor shafts.

An important factor influencing the correct performance of measurement and testing of belt drives is the correct belt tension. For this purpose, the belt drive is equipped with a tensometer sensor EMSYST EMS50 which is located between the plate 6 and sliding bed of steel base frame 1 (Figure 1b).

For the purpose of control, the operation of electric motors, the belt drive is equipped with a control and regulate unit B1 (Figure 1a, Figure 2) consisting of a pair of speed converters and a connection cable with a USB / RS485 converter, which enables to connect the speed converters to the computer.



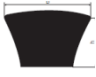
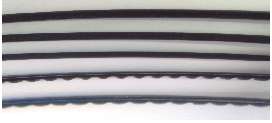
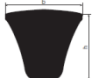
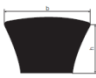
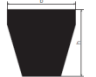
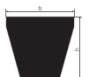
Figure 2: Detail of Control and Regulation Unit. 1 - Speed Converter of the Driver Electric Motor, 2 – Speed Converter of Driven Electric Motor, 3 - Box with Modular Breakers, 4 - Central Power Switch, 5 – Controlling Regulators.

The electric motors of the belt drive are controlled by a pair of Altivar 71 type ATV71HU15N4 frequency (speed) inverters from Schneider Electric. It is a frequency converter which regarding its properties and ease of use is designed for use in more difficult and complicated applications with power ranges of up to 500 kW. The basic characteristics of the Altivar 71 frequency converter includes the speed and power control capability even at low speed. It has many features such as PID controller, brake control suitable especially for conveyor systems, strokes and other applications. The control and regulation unit of the testing stand comprises the computer and software for the processing of received data.

2.1 V-belts

For this analysis, the belts were all assumed to be equivalent in wedge type (A), belt size (13), length (L_d 1480 – 1485) and set of operating conditions. The cross-section of V-belt is of trapezium shape. The cords as tension member with a high tensile strength provides and carries up to 95 % of the torque loading during the operation of the V-belt drive system. The rubber layers ensure frictional and absorbing shock properties and transmits the torque between the pulley and cords. The textile top cover (wrap) protect the V-belt during the V-belt drive system operation [12].

Table 1: Tested Belts

	Wedge	V-belt	Profile	Profile dimension [mm]	Weight[kg]	View
Belt 1	Classical wrap	Hi-Power 13x1475Li A58		13x8	0.190	
Belt 2	narrow wrap	Super HC SPA 1482		13x10	0.204	
Belt 3	classical wrap	Delta classic 13x1450Li/1480Ld A57		13x8	0.164	
Belt 4	Narrow cogged	Super HC MN SPA 1482 MN		13x10	0.154	
Belt 5	Narrow cogged	Quad-Power 4 XPA 1482		13x10	0.141	

The characteristics of tested belts are in Table 1. The twisted load-carrying tensile cords of tested V-belts are made of polyester and compression and tension parts of belts are made of polychloropren. Basically, the strength V-belts is achieved by reinforcing “fibers” – cords. Belts 1 – 3 are covered by rubberized fabric outer material. Belts 4 and 5 are of cogged construction. Belts 2, 4 and 5 are of narrow wedge. It means that tensile and load-carrying part of belt are the same as classical wedge, but compression part is larger.

2.2 Slip of Belt

The power of electric motor on input shaft is transmitted by belt. The part of belt that leaves the driven pulley and approaches the driven pulley is the tight side – tension T_1 , Figure 3. The belt is subjected to tension at the both sides (the slack side – tension T_2). The tensions are not the same in magnitude: $T_1 > T_2$.

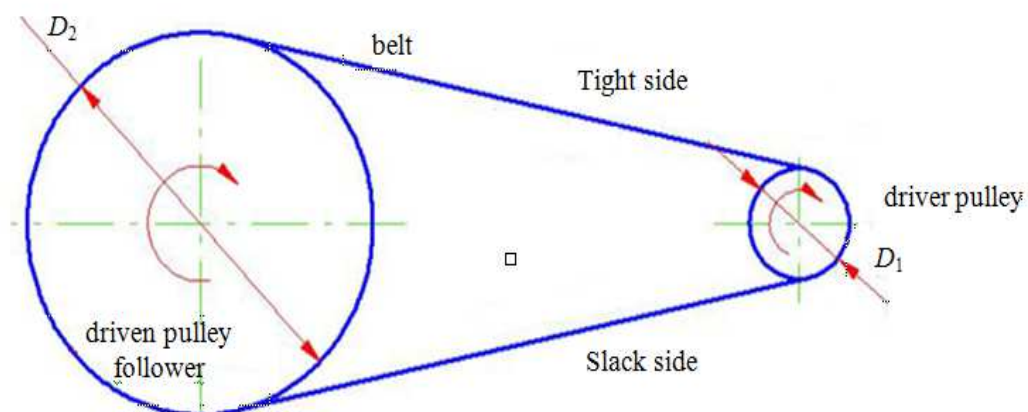


Figure 3: Schema and Description of Open Belt Drive in Figure 1b.

The measurement of slip was performed on the belt driver in Figure 1 (B and B1) and belt A 1150 Lw 13x1120 Li. When belt slips the velocities of belt and pulley are not the same. The belt does not move with pulley. It means the velocity of belt v_b is less than tangential velocity of driver pulley v_1 : $v_b < v_1$. Then:

$$v_b = v_1 - v_1 \frac{S_1}{100} = \pi D_1 n_1 \left(1 - \frac{S_1}{100} \right) \quad (1)$$

where S_1 is slip over the driver pulley, n_1 is speed of driver pulley and D_1 is diameter of driver pulley.

The speed is transferring to the driven pulley, but pulley cannot move this speed. Tangential velocity of driven pulley v_2 is less than velocity of belt v_b . Then:

$$v_2 = v_b - v_b \frac{S_2}{100} = v_b \left(1 - \frac{S_2}{100} \right) \quad (2)$$

where S_2 is slip over the driven pulley.

When submitting equation (1) to (2), we obtain:

$$v_2 = \pi D_1 n_1 \left(1 - \frac{S_1 + S_2}{100} \right) = \pi D_2 n_2 \quad (3)$$

where n_2 is speed of driven pulley and D_2 is diameter of driven pulley.

Resulting from (3), we obtain the velocity ratio in terms of slip:

$$\frac{n_2}{n_1} = \frac{D_1}{D_2} \left(1 - \frac{S}{100} \right) \quad (4)$$

where n_1 and n_2 is speed of driver and driven – follower pulley (rpm), respectively, D_1 and D_2 is diameter of driver and driven pulley, S is total slip in the driver (%): $S = S_1 + S_2$, where S_1 and S_2 is slip over the driver and driven pulley.

Not considering the slip, the velocity ratio is:

$$\frac{n_2}{n_1} = \frac{D_1}{D_2} \quad (5)$$

Then theoretical gear ratio i_T :

$$i_T = \frac{D_2}{D_1} = \frac{160\text{mm}}{80\text{mm}} = 2 \quad (6)$$

where D_2 is diameter of larger – driven pulley and D_1 is diameter of smaller – driver pulley in Figure, 1b.

Theoretical speed of driven electromotor n_{2T} :

$$n_{2T} = \frac{n_{1T}}{i_T} = \frac{1600\text{rpm}}{2} = 800\text{rpm} \quad (7)$$

In following part, the example of the belt slip calculation is provided. If the measured speed, i.e. real speed, of driven pulley is $n_{2R} = 780\text{rpm}$, then the slipspeed Δn_2 is:

$$\Delta n_2 = n_{2T} - n_{2R} = 800\text{rpm} - 780\text{rpm} = 20\text{rpm} \quad (8)$$

Time of sliding T :

$$T = \frac{60}{\Delta n_2} = \frac{60}{20\text{rpm}} = 3\text{s} \quad (9)$$

The specific belt slip ξ :

$$\xi = \frac{60}{T \cdot n_{1R}} i_T = \frac{60}{3\text{s} \times 1600\text{rpm}} \times 2 = 0.025 \quad (10)$$

The real and theoretical speed of driven pulley are the same: $n_{1R} = n_{1T}$.

The coefficient of belt elastic creeping Ψ :

$$\Psi = 1 - \xi = 1 - 0.025 = 0.975 \quad (11)$$

The real gear ratio i_R :

$$i_R = \frac{D_2}{D_1 \Psi} = \frac{i_T}{\Psi} = \frac{2}{0.975} = 2.0513 \quad (12)$$

3. RESULTS AND DISCUSSIONS

3.1 Vibration and Temperature Measurement Results

During testing, as the operating conditions we consider the sequential measurements in different operational modes in following order: tensioning force 400 N, load of driven electric motor (machine) 0%, rotational speeds 600, 1200, 2000 and 3000 rpm, 40% - 600, 1200, 2000 and 3000 rpm, 75% 600 rpm a 100% - 600 rpm and the same modes order for tensioning force 700N. The number of mentioned measurements (operational modes) was 20. In some cases, (belts 1, 2, 3), at a load of 70 and 100%, the measurements could also be made at 1200 rpm. Thus, the maximum number of measurement was 22.

The results of RMS (root mean square) vibrational velocity in whole range of rotational speed for load 0 and 40% are in Figures 4 and 5 and for load 70 and 100% measured for 600 rpm are in Table 2. Values in Table 2 are low comparing to maximum vibrational velocity about 0.325 m/s in Figures 4 and 5. Maximum vibrational velocities are for 2000 rpm and belts 2 and 4.

Table 2: RMS of Vibrational Velocity for 600 rpm and Load on Driven Pulley 70 % and 100 %

Belt 1	70%	100%
400N	0.086975	0.086698
700N	0.075812	0.091494
Belt 2	70%	100%
400N	0.108741	0.045023
700N	0.041702	0.028913
Belt 3	70%	100%
400N	0.101432	0.07953
700N	0.055852	0.0611
Belt 4	70%	100%
400N	0.028289	0.051529
700N	0.089146	0.033888
Belt 5	70%	100%
400N	0.165988 (max.)	0.005774 (min.)
700N	0.052711	0.046463

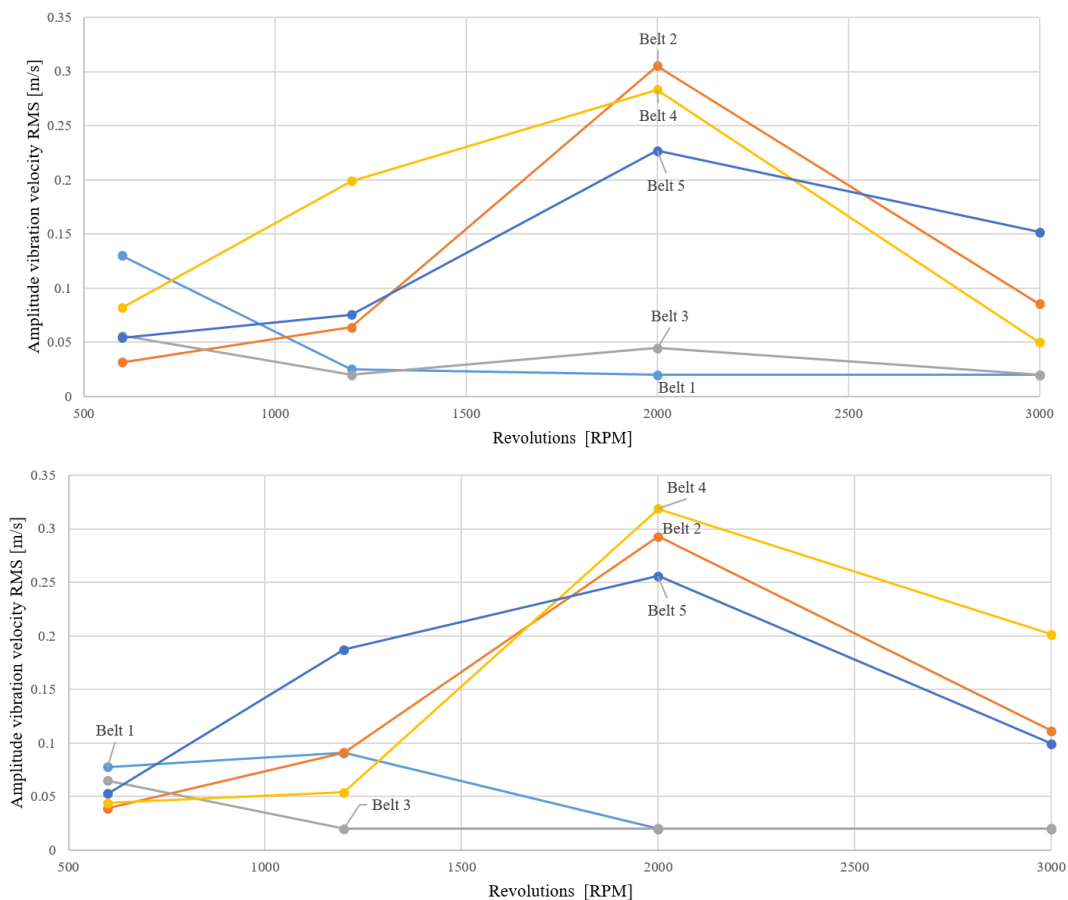
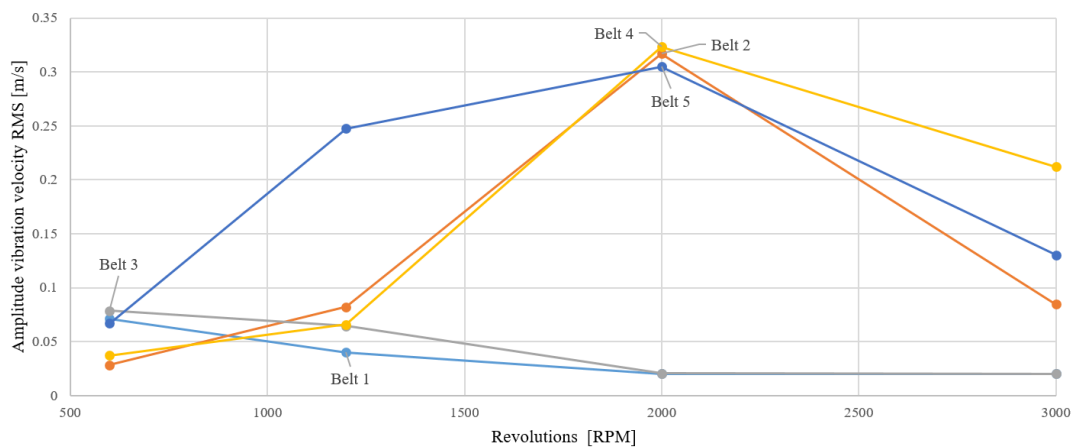


Figure 4: RMS of Amplitude Vibrational Velocity for Tension Force 400 N and Load on Driven Pulley 0% (up) and 40%

Observing the results in Figures 4 and 5, the very similar dynamic behaviour can be observed for belts 1 and 3, 2 and 4. Belt 5 has a different behaviour but close to behaviour of belts 2 and 4. The maximum vibrational velocities values are for belts 2 and 4 running 2000 rpm. This is probably a resonant belt area. For other rotational speeds, the vibrational velocity is several times lower. Furthermore, similar dynamic behaviours have belts 1 and 3 in which operation is very stable (average 0,059 and 0,042 m/s) in a small range of vibrational velocity values.



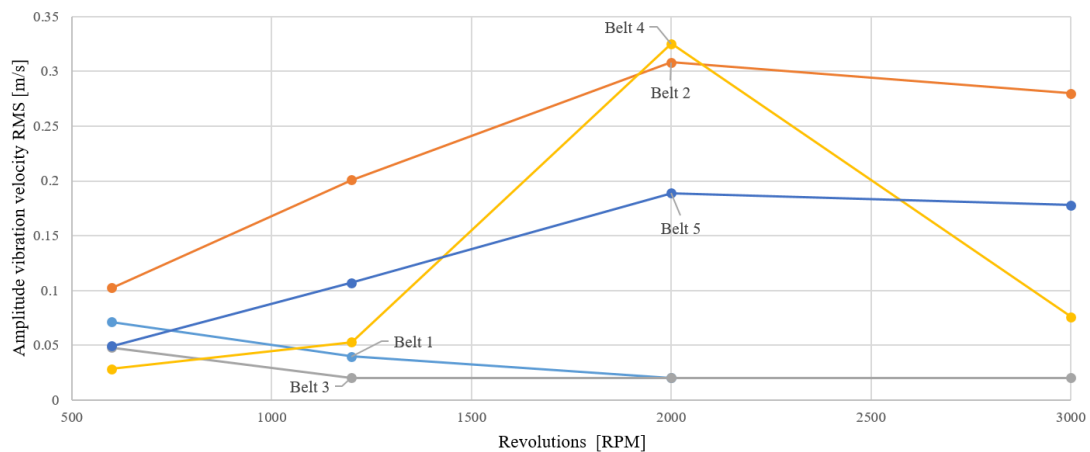


Figure 5: RMS of Amplitude Vibrational Velocity for Tension Force 700 N and Load on Driven Pulley 0% (up) and 40%.

Considering only the vibration behaviour, belts 1 and 3, i.e. belts with a classical cross-section are the most suitable. However, taking into account the temperature and the temperature change (Figures 6) during running, it can be observed that belts 1 and 3 reach the highest temperatures and the temperature change (along with belt 2).

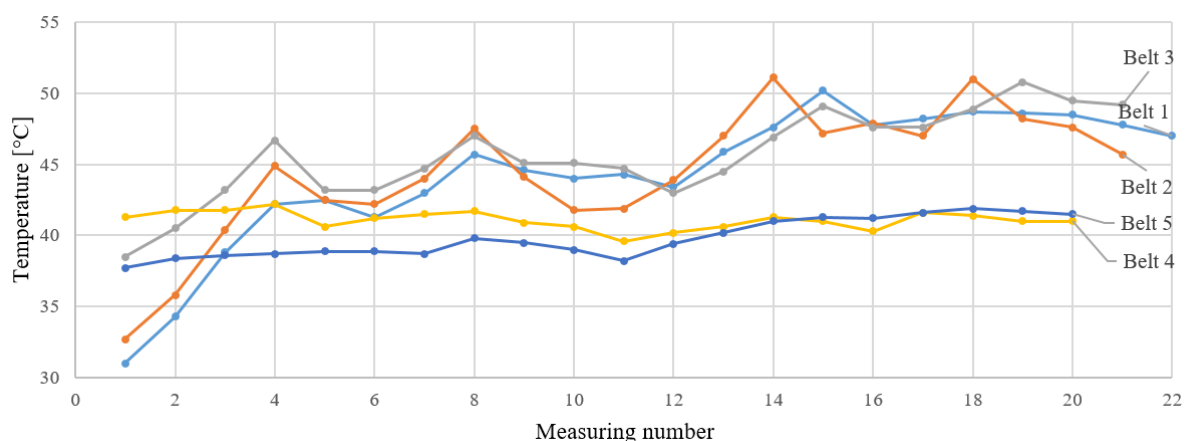


Figure 6: Temperature.

The results of the temperature curves are very interesting for belts 4 and 5. Belts 4 and 5 besides being cogged also have a narrow profile. In the belt 4, there is no temperature change comparing the first and last operational modes. For belt 5, this change is only 3.8°C, figures. 6, 7. For belt 1, there is the largest temperature change of 16°C, as figure 7 shows along with the distribution of the temperature at the first and last of the measured operational modes. For belts 2 and 3, the temperature change is 13 and 10.2°C, respectively.

The source of high-positive thermal behaviour of belts 4 and 5 are cogs which reduce the contact area and slip between the pulley groove and the belt and reduce heat built-up and thereby extends the belt life. Moreover, comparing belt weight (Table 1), belts 4 and 5 are of the least weight. Further, the edges of belts 4 and 5 are not wrapped, thus have a higher coefficient of friction and transmit more power. However, a higher coefficient of friction can be a disadvantage for operating conditions with peaks of the torsion moment when the sides of the belt are more loaded compared to the wrap edge belts designed for better slip. Thus cogged belts are worn faster. The disadvantage of cogged belts is also in case of abrasives in working environment. The abrasives placed between the pulley groove and the belt contribute to wear. For wrap

belt, this phenomenon is not significant as wrap belt sides are designed to allow slip. The cogged belts are more expensive. However, given belt size can transmit higher power so fewer number of belts (grooves) are required for the given load. The cogged belts with narrow profile are more flexible thus the small pulleys and less material to drive can be used and lower bearing load applied.

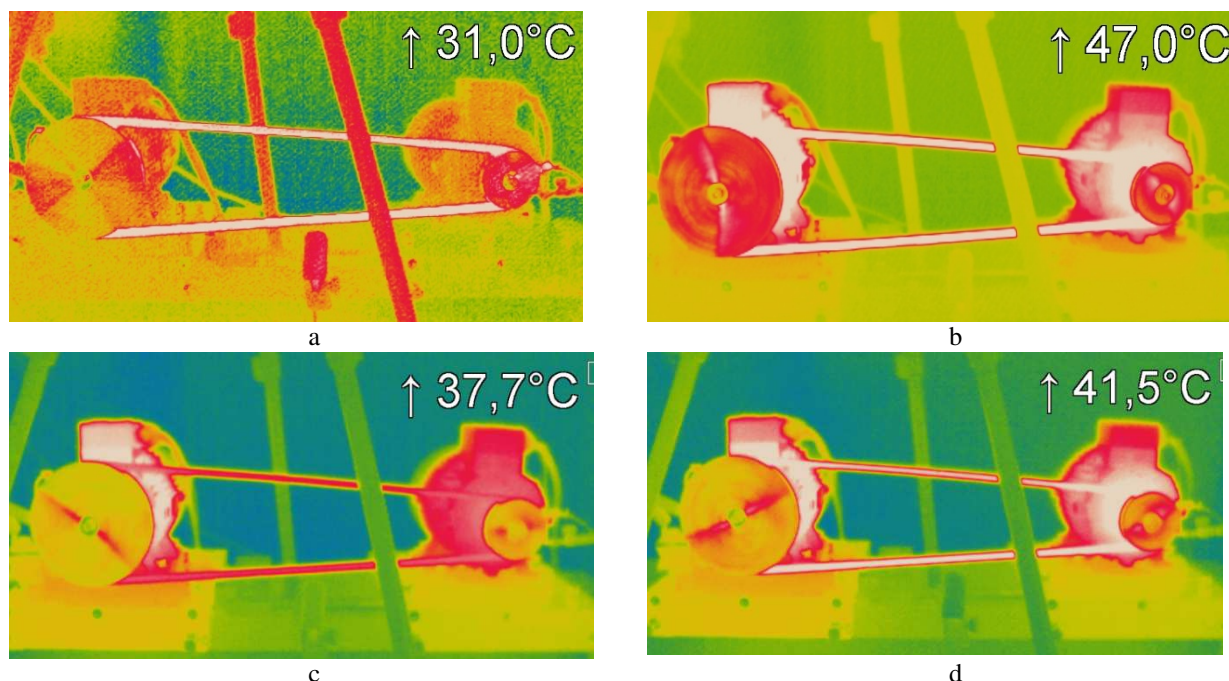


Figure 7: Temperature Change of Belt 1: $\Delta t = 16^\circ\text{C}$; belt 5: $\Delta t = 3.8^\circ\text{C}$ first (a, c) and Last (b, d) running Modes.

3.2 Belt Slip Measurement Results

The measurement of slip was made for the V-belt A 1150 Lw 13x1120 Li and with tensioning force set at 150N. Next step necessary to carry out the measurement and completion of the resulting slip value and other variables was to start the driving and driven electric motors and to define the required values for the driving electric motor speed and the torque on the driven electric motor. The required parameters were defined by frequency converters. The measurement of slip was made for 25, 50 and 60% of the electric motor load obtained by control of electric motor on the driven side. Moreover, the belt slip was measured at speed 1300, 1600 and 2000 rpm.

The known input parameters were entered into the software “Motor”. These parameters include the electric motor speed, the theoretical gear ratio calculated as a ratio the driver and driven pulley diameters is 0.5 (gear ratio according to (6) is 2 so the gear reduction is 1:2). The set input values for a given measurement are shown in figure 8.

After the initial setting of the required input parameters, the slip measurement process continued by scanning the real speed of the driver and driven electric motors. These data were sent from the sensors to an analog-to-digital converter where they were converted and further sent to the computer where they were evaluated by the Motor software.

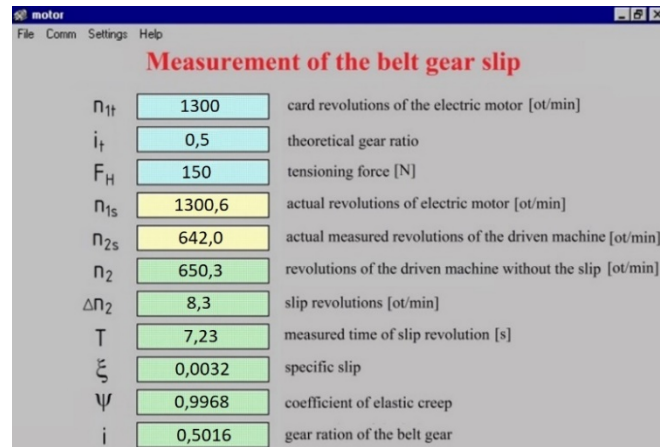


Figure 8: The Measurement Input Values and Results of Belt Drive Slip in Motor Software.

The comparative parameter belonging to the principal indicators of slip is specific belt slip ξ or the belt elastic creeping coefficient ψ . The curves formed by the measured specific belt slip ξ values (Figure 9) are slightly increase while increasing the speed of driver pulley (electric motor) n_1 . Moreover, the increasing the load from 25 to 60%, the specific belt slip decreasing, supposing that it depends on tensioning force.

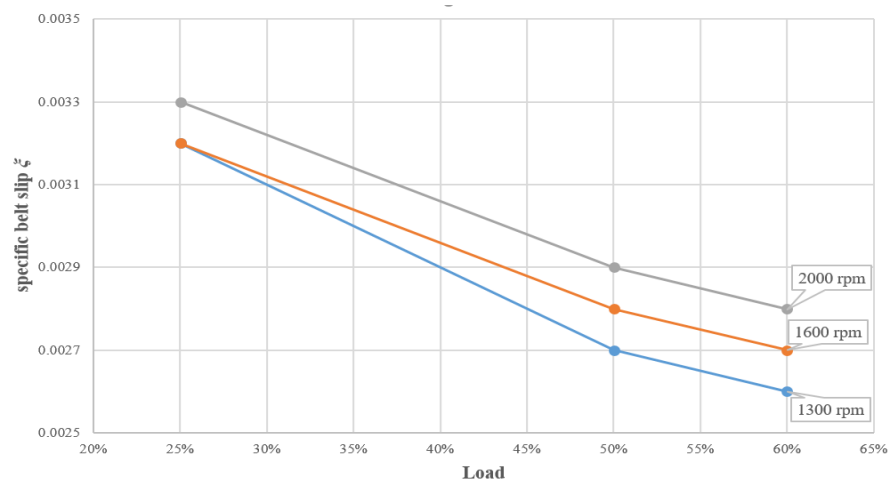


Figure 9: Measured Specific Belt Slip.

Table 3 shows other measured and calculated values according to equations (6)-(12).

Table 3: Results for Theoretical Speed 1600 rpm

n_1 [rpm]	n_{2T} [rpm]	n_{1R} [rpm]	n_{2R} [min ⁻¹] [rpm]	Δn_2 [rpm]	T [s]	ξ	ψ	i	load [%]	M_T [Nm]
1600	800	1601.7	790.5	10.4	5.8	0.0032	0.9968	2.0261	25	1.25
1600	800	1601.6	791.7	9.1	6.59	0.0028	0.9972	2.0230	50	2.5
1600	800	1600	792.2	8.8	6.86	0.0027	0.9973	2.0197	60	3

4. CONCLUSIONS

In this study we examined performance of different belts of the same wedge type, belt size and length. We examined influence of the shape of the profile (classical and narrow), wrap and cogs and the various operating conditions that varying speed, load, belt tensioning force. The vibrational behaviour was better for wrapped belts 1 and 3 with classical profile with a very stable running but with a considerable increase in temperature. In contrary, the best temperature

behaviour was for narrow profiled and cogged belts 4 and 5, but with significant vibrations in rotational speed 2000 rpm. Taking into account together RMS vibrational velocity, temperature and temperature change, the best performance is for belt 4, followed by 5, 3, 1 and worst results are for 2.

Moreover, the study examined the specific belt slip as important parameter for estimation of effectivity of belt drive that depends on driver speed and load of driver. If the load increases, the specific belt slip also increases.

ACKNOWLEDGMENTS

The authors would like to thank the Agency of Ministry of Education, Science, Research and Sport of the Slovak Republic for supporting this research: grant VEGA 1/0910/17.

REFERENCES

1. Nakashima, E., & Okuno, S. (2015). U.S. Patent No. 8,974,336. Washington, DC: U.S. Patent and Trademark Office;
2. Ishiguro, H., Takano, K., & Miura, Y. (2018). U.S. Patent No. 10,001,193. Washington, DC: U.S. Patent and Trademark Office.
3. Okubo, T., Takahashi, S., & Kawahara, H. (2019). U.S. Patent Application No. 10/323,717; Miyata, H., Nakane, S., & Izumi, H. (2018). U.S. Patent Application No. 10/000,029;
4. Michalik, P., & Zajac, J. (2012, May). Using of computer integrated system for static tests of pipe conveyor belts. In *Proceedings of the 13th International Carpathian Control Conference (ICCC)* (pp. 480-485). IEEE.
5. Silva, C. A., Manin, L., Andrianoely, M. A., Besnier, E., & Remond, D. (2019). Power losses distribution in serpentine belt drive: Modelling and experiments. *Proceedings of the Institution of Mechanical Engineers, Part D: Journal of Automobile Engineering*, 0954407018824943.
6. Reddy, K. S., & Dufera, S. *Additive Manufacturing Technologies. Best: International Journals of Management, Information Technology and Engineering (BEST: IJMITE)*, ISSN (P), 2348-0513.
7. Winczek, J. (Ed.). (2018). *Selected Problems of Contemporary Thermomechanics. BoD—Books on Demand*.
8. Lubarda, V. A. (2015). Determination of the belt force before the gross slip. *Mechanism and Machine Theory*, 83, 31-37.
9. Kong, L., & Parker, R. G. (2005). Microslip friction in flat belt drives. *Proceedings of the Institution of Mechanical Engineers, Part C: Journal of Mechanical Engineering Science*, 219(10), 1097-1106.
10. Shieh, C. J., & Chen, W. H. (2002). Effect of angular speed on behavior of a V-belt drive system. *International journal of mechanical sciences*, 44(9), 1879-1892.
11. Gandhi, P. P., & Sharma, G. *The pallet conveyor system application in the industrial lines—a new design system with improvement of productivity*.
12. Reynolds, O. (1875). On the efficiency of belts or straps as communicators of work. *Journal of the Franklin Institute*, 99(2), 142-145.
13. Gerbert, G., (1996) *Belt slip—a unified approach*. 432-438.
14. Shieh, C. J., & Chen, W. H. (2002). Effect of angular speed on behavior of a V-belt drive system. *International journal of mechanical sciences*, 44(9), 1879-1892.
15. Venkategowda, T., & LH, M. *Free vibration characteristics of alkali treated unidirectional long kenaf fiber reinforced epoxy composites at various end conditions*.

AUTHOR'S PROFILES



Assoc. Prof. MSc. Zuzana Murčínková, PhD. is an associate professor in the field of Production Machinery. She focuses on the fields of applied mechanics, production machinery, manufacturing technologies, mechanics of materials, static and dynamic simulation of mechanical behaviour of structures using the finite element method. These fields of research are multidisciplinary joined in the field of applications, computational methods, design and testing of composite materials. She is the lead author and co-author of 11 scientific papers in Current Content journals, 1 monography in renowned foreign publishers, 3 chapters in scientific monographs in renowned publishers, 3 university textbooks and 81 scientific papers in the Web of Science and Scopus databases and 148 citations in Web of Science and Scopus databases.



MSc. Jozef Maščenik, PhD. His research activity was focused on the production of teeth by unconventional technologies and design of parts of machines, mechanisms and construction nodes. Recently, his research is in the field of belt drives testing under various conditions and extreme loads.



RNDr. Tibor Krenický, PhD. deals with the following activities: design and implementation of experimental devices using virtual instrumentation, multi parametric measurement of physical quantities, evaluation of diagnostic parameters, especially in the field of vibro-diagnostics. He has good experience with the creation of innovative experimental sets for measuring quantities under controlled conditions and for processing diagnostic data.

ŠTEFAN GAŠPÁR-



MSc. Štefan Gašpár, PhD. is an associate professor in the study branch Manufacturing Technologies. His research activity is focused on the research of influence of technological factors of pressure casting on the mechanical properties of pressed casting. Recently, he has been dealing with the use of robotic systems in the production process, mathematical formulations of kinematic equations for robotic systems management, and the development of non-traditional planetary gears.



MSc. Ján Paško, CSc. is a professor in the study branch Manufacturing Technologies. His research activity is focused in influence of die casting factors, improving production efficiency and mechanics of continuum.